ELSEVIER

Journal of Fluids and Structures 26 (2010) 160–175

JOURNAL OF FLUIDS AND STRUCTURES

www.elsevier.com/locate/jfs

Optimal lift force coefficient databases from riser experiments

H. Mukundan*, F. Chasparis, F.S. Hover, M.S. Triantafyllou

Center for Ocean Engineering, Massachusetts Institute of Technology, 77 Massachusetts Avenue, Cambridge, MA 02139, USA

Received 30 September 2008; accepted 9 September 2009
Available online 27 November 2009

Abstract

Significant past effort has gone into understanding the complicated flow–structure interaction problem of vortex-induced vibration (VIV) of long flexible cylindrical structures (e.g., risers, mooring lines, tendons, conductors) in the ocean environment. However, major challenges persist with regard to riser VIV modeling and response prediction. The existing prediction schemes are based on a number of hypotheses, experimental facts and data like strip theory, energy balance, correlation length and, most importantly, the use of lift force coefficient databases. Recent advances in observing the VIV motions on experimental risers with high confidence shows that some of these assumptions may not be valid. One important source of the discrepancies between theoretical estimates and experimental observations arise from the use of experimentally obtained lift coefficient databases. These databases were obtained under the laboratory conditions of limited Reynolds number, and under the assumption that the cross-flow motions are not influenced by restraining the in-line motions. In this paper we develop a method to improve the modeling capability of riser VIV by extracting empirical lift coefficient databases from field riser VIV measurements. The existing laboratory-based lift coefficient databases are represented in a flexible parameterized form using a set of carefully chosen parameters. Extraction of the lift coefficient parameters is posed as an optimization problem, where the objective is to minimize the error between the prediction using a theoretical model and the experimental data. Application of the method to data from the Norwegian Deepwater Programme experiments shows that the new optimal databases significantly reduce the error in estimating the riser VIV cross-flow response.

Keywords: Vortex-induced vibration; Marine risers; Lift coefficient databases; Optimization; Database extraction; Peak response frequencies; Peak response modes

1. Introduction

Consideration of vortex-induced vibration (VIV) of long flexible cylindrical structures enduring ocean currents like risers, tendons, mooring lines has become critical in the offshore industry since it affects significant design decisions like types of members used, dimensions of the members, arrangement of the members, choice of VIV suppression devices, and fabrication, installation and instrumentation details. As a result, the economic impact of quantifying and countering VIV in marine installations are significant. Thus, it is important to study and predict the response of such structures undergoing VIV.

*Corresponding author. Tel.: +1 857 928 2186.
E-mail address: harishm@alum.mit.edu (H. Mukundan)

0889-9746/$ - see front matter © 2009 Elsevier Ltd. All rights reserved.
doi:10.1016/j.jfluidstructs.2009.09.004

The ideal approach for quantifying the complicated problem of VIV (flow–structure interaction) would be the use of computational fluid dynamics (CFD) techniques; refer to Kaiktsis et al. (2007) and Sarpkaya (2004) for details. CFD methods when used with the appropriate mesh size can take into account the complicated wake around the riser. However, a full 3-D simulation of a riser at realistic Reynolds numbers is prohibitive due to the intensive computational requirements.

At present, the most widely used methods for predicting the riser VIV fatigue life are the empirical prediction schemes like VIVA [described in Triantafyllou et al. (1999)], SHEAR7 [described in Vandiver (2003)] or VIVANA [described in Larsen et al. (2005)]. Such an empirical scheme typically consists of two parts: (a) the empirical models and (b) the empirical databases. The important empirical models are the hydrodynamic models, the structural dynamic models, and the fatigue damage models. The empirical databases on the other hand primarily contain hydrodynamic information in the form of the lift force coefficients (*lift coefficient in phase with velocity* $C_{lv}(V_r, A^*)$ and *added mass coefficient* $C_m(V_r, A^*)$) and drag coefficients ($C_d(V_r, A^*)$). These force coefficients (refer to Fig. 1) are usually obtained from extensive laboratory experiments using an elastically mounted rigid cylinder [refer to Gopalkrishnan (1993)] and are functions of the nondimensional amplitude $A^* = A/D$ (A is the amplitude of oscillation) and nondimensional frequency of oscillation $V_r = U/fD$ (f is the frequency of oscillation) of the response in the cross-flow (CF) direction.

Alternatively, we can view the problem at hand from a systems perspective. The problem of obtaining the vortex-induced CF response of a riser can be subdivided into a *hydrodynamics subproblem* which quantifies the action of the fluid (surroundings) on the structure (system), and secondly a *structural dynamics subproblem*, which predicts the response of the system given excitation from the fluid. From a hydrodynamic viewpoint, both the magnitude and the direction of the steady current may change along the riser span. This leads to significant variation in the magnitude, direction and frequency of the vortex-induced forces along the length of the structure. It is a common practice [refer to Triantafyllou et al. (1999), Vandiver (2003)] to use a strip theory based (quasi-uniform) approach to subdivide the riser into smaller segments which act like elastically mounted rigid cylinders and estimate the vortex-induced forces on each of these segments. The harmonic part of the vortex-induced forces on a cylinder segment corresponding to a local flow velocity U and density ρ_f reduces to estimating its two components; the *excitation force in phase with velocity* and the *excitation force in phase with acceleration* [refer to Sarpkaya (1979), Gopalkrishnan (1993), Triantafyllou (1998)]. As shown by Triantafyllou (1998), estimating these forces requires empirical lift coefficient databases of *added mass coefficient* $C_m(V_r, A^*)$ and *lift coefficient in phase with velocity* $C_{lv}(V_r, A^*)$. From a structural dynamics viewpoint, a riser is adequately modeled as a tensioned beam with the appropriate boundary conditions, acted upon by the external hydrodynamic force. Since VIV is a self-limited process with small amplitudes of motions, the riser structural dynamic model is assumed to be linear. This linear structural dynamics model is used to obtain the riser response once we quantify the forces acting from the fluid on the structure. The hydrodynamic force, however, depends on the riser motions themselves and thus the above two problems are coupled. So, an iterative scheme which goes back and forth between the hydrodynamics and structural dynamics subproblems is needed to evaluate the riser response. The problem is made rich due to the challenging hydrodynamics, where the wake results in a net force from the fluid to the riser (an excitation region), or from the riser to the fluid (damping region), or even forces which travel along the riser due to the formation of vortex streets sheared off from the riser [described in Williamson and Roshko (1988), Khalak and Williamson (1996, 1999), Govardhan and Williamson (2000)].

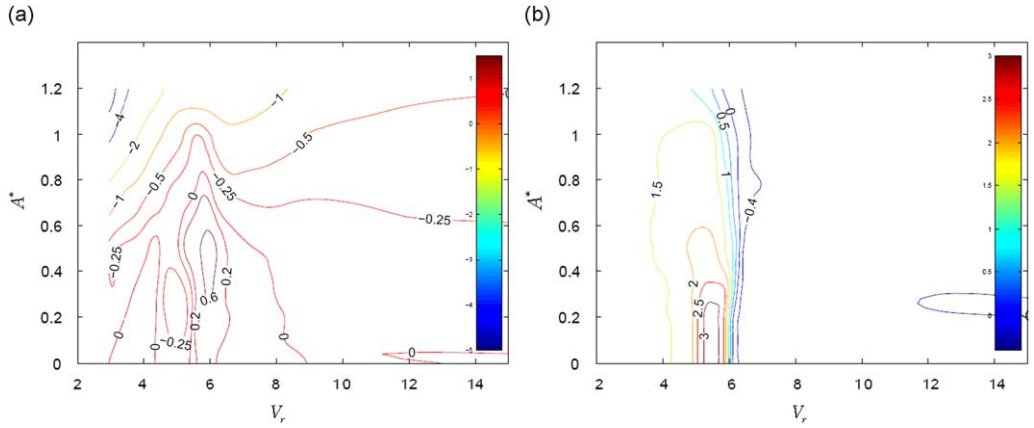

Fig. 1. The extensive C_{lv} and C_m database obtained by Gopalkrishnan (1993). (a) $C_{lv}(V_r, A^*)$ and (b) $C_m(V_r, A^*)$.

The presently available extensive C_{lv} and C_m databases were obtained by Gopalkrishnan (1993) and Smogeli et al. (2003) from simplified laboratory-scale experiments (performed at the MIT towing tank) where a cylinder was forced to oscillate at prescribed trajectories at given frequencies and amplitudes of oscillation at a specific Reynolds number regime. For detailed description refer to Hover et al. (1998), Gopalkrishnan (1993), and Vandiver (1998). However, these databases were obtained by Gopalkrishnan (referred to as the *nominal databases*) under certain conditions: (i) databases are available for limited Reynolds number regimes; (ii) cylinders undergo simplified motion tests at a single frequency; (iii) cylinder motions are restricted to cross-flow (CF) direction instead of both cross-flow and in-line (IL) motions. It has been observed from various field experiments (Smogeli et al., 2003) that the C_m and C_{lv} databases for increased Reynolds number will preserve all the major features (peaks and valleys) in the database, but these features are found to move and scale (a *warping transformation*). In a similar manner, allowing IL motions has the effect of *adding another peak* in the C_{lv} database (Marcollo and Hinwood, 2006). Recent improvements in estimating the vortex-induced motion of an entire marine riser using data from a limited number of sensors [refer to Mukundan et al. (2008a)] have improved our capability to closely observe and reverse engineer the hydrodynamic data. However, obtaining similar extensive databases from field experimental data is not straightforward and it is often possible to construct a small subset of all the combinations of V_r and A^* available in the Gopalkrishnan databases.

Due to the above-mentioned limitations, the response predicted by empirical programs (VIVA, SHEAR7, VIVANA) differ significantly from observations from the field experiments as shown by Chaplin et al. (2005). To overcome these limitations, there is a need to develop a method which can extract information from more realistic experiments [e.g., Norwegian Deepwater Programme (NDP) experiment (Braaten and Lie, 2004), Gulf stream test (Vandiver et al., 2006a)] and build on the presently available extensive databases of $C_m(V_r, A^*)$ and $C_{lv}(V_r, A^*)$. The method we develop should be able to understand and preserve the key features of the $C_m(V_r, A^*)$ and $C_{lv}(V_r, A^*)$ databases important to accurately predicting the VIV response of the riser. It would be very beneficial to design the scheme so as to minimize extensive changes to the presently available VIV prediction programs.

This paper is structured as follows: in Section 2 we state the problem, present the working hypothesis and provide a brief overview of the solution scheme. Next, in Section 3 we describe the available experimental measurements and how we can predict the corresponding theoretical quantity. Section 4 poses the problem of extracting the lift coefficient databases as a parameter estimation problem. A method to find the universal databases from several optimal databases (corresponding to each NDP dataset) obtained for a family of linearly sheared datasets from the NDP is discussed in Section 5. Finally Section 6 concludes the paper by providing a summary of the overall scheme and the key contributions.

2. Problem statement and solution overview

We will assume that the models used for predicting the response are accurate, while the discrepancy between predictions and measurements arise from the uncertainty in the empirical databases alone. We aim at systematically modifying the nominal lift coefficient databases of $C_m(V_r, A^*)$ and $C_{lv}(V_r, A^*)$ to take into account the effects of (i) higher Reynolds number regimes; and (ii) allowing IL and CF motions. The modifications of the databases are to be performed so that predictions from a semi-empirical program like VIVA using the modified databases most closely match the experimentally observed results.

An ideal approach would employ two sets of data (training-dataset and test-dataset). The training-dataset to extract the lift coefficients, and the test-dataset to independently verify the quality of the resulting prediction. Due to insufficient experimental data available to us, such a complete test of the predictive capability is not feasible. In this paper, our aim is to formulate the lift coefficient extraction as a well-defined problem, provide a suitable solution technique, and apply it to one set of experimental data.

2.1. Working hypothesis

The working hypothesis for correcting the databases is based on the observations of various researchers mentioned previously; refer to Smogeli et al. (2003), Marcollo and Hinwood (2006), and Venugopal (1996). Based on these observations, we assume that we can obtain modified databases which will account for the discrepancy between the measurements and the predictions. The modifications we propose are as follows:

(i) correction for high Reynolds number → warping of the nominal C_m and C_{lv} databases;
(ii) correction for allowing in-line motions → adding another peak in the C_{lv} database.

2.2. Solution overview

Appropriately parameterizing the relevant features of the databases using a chosen set of parameters $\vec{p}$ will allow these databases to be flexible (allowing for warping and a second peak). Hence, the flexible databases created can absorb the hydrodynamic information from the experimental data. The theoretical predictions using these modified C_m and C_{lv} databases will be compared with the experimentally observed riser response and the discrepancies will be understood.

As a first step, we will specifically identify (define) the experimental measurements which will be compared with the theoretical estimates. This will be followed by a careful explanation of the key features of the C_m and C_{lv} databases which determine the theoretical estimates. Next, we will pose the problem of extracting the improved databases as an optimization problem, where the C_m and C_{lv} databases are parameterized using a chosen set of parameters $\vec{p}$. The optimization problem requires an optimization index or error metric which will be defined. The choice of the appropriate solution technique will be discussed, which will be followed by the development of a method to obtain the universal C_{lv} and C_m databases which minimize the overall error over a family of NDP datasets.

3. Experimental measurements and theoretical estimates

For a simple single degree of freedom (SDOF) system like an elastically mounted rigid cylinder, the input is the flow velocity U and the observables are the peak response amplitude A and the peak response frequency ω. In a similar fashion, a distributed system like a riser has, as input, a steady velocity profile $U(z)$ in the in-line direction, and, as observables, the set of excited *peak response frequencies* ω_n and the corresponding set of *peak response modes* $Y_n(z)$. As a result, while formulating a comparison of the riser CF response both ω_n and $Y_n(z)$ are important. The methods to obtain ω_n and $Y_n(z)$ from experimental data and the corresponding theoretical estimates will be described in the next sections.

3.1. Experimental measurements

In this paper we use data from a set of high mode VIV tests by the Norwegian Deepwater Programme (NDP) described in detail by Braaten and Lie (2004). The riser model was taut horizontally and towed in water in a testing tank at various flow speeds to obtain a family of uniform velocity flow profiles ($U(z) = U_{\max}$) and a family of linearly sheared flow profiles ($U(z) = U_{\max}(1 - z/L)$). For a uniform flow profile, both ends of the riser model were towed simultaneously with a velocity $U_{\max}$, while a linearly sheared flow profile was obtained by towing one end of the riser in a circular arc with a velocity $U_{\max}$ while keeping the other end at rest. The riser model, made of fiberglass, had the following properties: length $L = 38$m, diameter $D = 0.027$ m, linear mass density in air $m = 0.761\,\mathrm{kg\,m^{-1}}$, tension $T = 5000$ N (assumed value, the actual value varied between $T = 4000$ and 6000 N) and bending stiffness $EI = 37.2\,\mathrm{N\,m^2}$. The riser was instrumented with 24 strain gages and eight accelerometers which were used to measure the CF response of the riser.

A detailed description of the theory and methodology for obtaining the peak response frequencies $\omega_{n-\mathrm{ex}}$ and peak response modes $Y_{n-\mathrm{ex}}(z)$ from experimental data is provided in Mukundan (2008). Here, we provide only a brief description of the procedure, which is illustrated by the flowchart given in Fig. 2. Given experimental data from sensors located along the riser, we identify a statistically stationary segment of experimental data using scalograms (Mukundan et al., 2008b). A response reconstruction is then performed to obtain the displacement time series at any point along the riser $y(z,t)$ [refer to Mukundan et al. (2008a)] using the Fourier decomposition method, as it allows for confidence during the reconstruction. We compute the Fourier transform of the time signals at every location along the span to obtain the Fourier coefficients $\hat{y}(z,\omega)$. Note that there are some intermediate signal processing steps like windowing of the time series. These steps require that we are able to obtain several cycles of the measured riser VIV within the extracted statistically stationary region of the riser response. The set of peak response frequencies $\omega_{n-\mathrm{ex}}$ are obtained

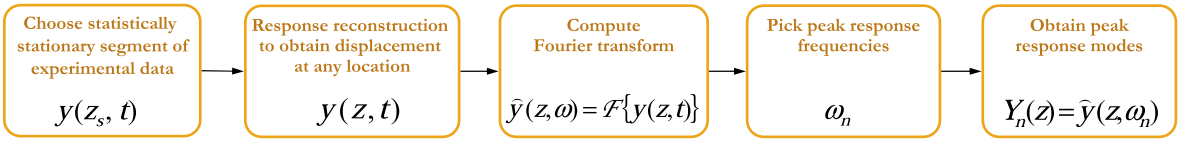

Fig. 2. A flowchart describing our method to obtain the peak response frequencies and the peak response modes from experimental data.

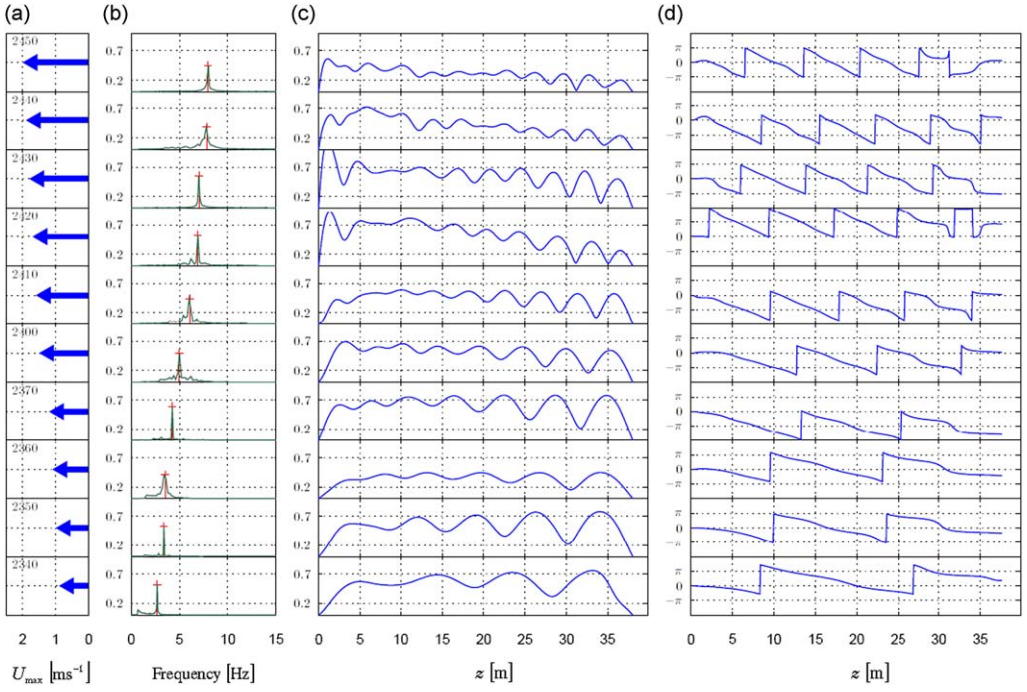

Fig. 3. Modal decomposition of the riser response for several linearly sheared flow profile datasets (each row corresponds to one dataset) from NDP experiments. (a) The maximum velocity $U_{\max}$ for various NDP datasets; (b) the harmonic part of the span averaged displacement spectra for various NDP datasets; (c) the peak response modal magnitudes for various NDP datasets; (d) the peak response modal phase angles for various NDP datasets.

from the peaks of a span averaged spectrum of the response. Finally, the corresponding peak response modes $Y_{n-\mathrm{ex}}(z)$ are obtained by extracting the Fourier coefficients corresponding to each peak frequency along the entire riser.

Using this method, we obtain a library of peak response modes and peak response frequencies (refer to Fig. 3) corresponding to a family of NDP datasets corresponding to a triangular flow profile of the form $U(z) = U_{\max}(1 - z/L)$ depicting a single frequency of peak response.

3.2. Theoretical estimates

A detailed derivation for obtaining the theoretical estimates of the peak response frequencies $\omega_{n-\mathrm{th}}$ and the peak response modes $Y_{n-\mathrm{th}}(z)$ can be found in Triantafyllou (1998). In short, given the velocity profile $U(z)$, the lift coefficient databases of C_m and C_{lv}, and the appropriate boundary conditions the theoretical estimates of peak response frequencies $\omega_{n-\mathrm{th}}$ and peak response modes $Y_{n-\mathrm{th}}(z)$ are obtained by solving the nonlinear eigenvalue problem:

$$\left\{-\omega^2\left[m + C_m\left(\rho_f \frac{\pi D^2}{4}\right)\right] + i\omega b\right\} Y - \frac{\partial}{\partial z}\left(T\frac{\partial Y}{\partial z}\right) + \frac{\partial^2}{\partial z^2}\left(EI\frac{\partial^2 Y}{\partial z^2}\right) = iC_{lv}\left(\frac{\rho_f U^2}{2} D\right)\frac{Y}{|Y|}, \tag{1}$$

where D is the riser diameter, b is the linear structural damping coefficient, T is the assumed tension, m is the linear mass density in air, EI is the bending stiffness and ρ_f is the density of the fluid. The empirical prediction program VIVA described in Triantafyllou et al. (1999) can solve the nonlinear eigenvalue problem given by Eq. (1), and we use it to evaluate the theoretical estimates $Y_{n-\mathrm{th}}(z)$ and $\omega_{n-\mathrm{th}}$.

In a more complicated setting of realistic risers where computing the experimentally obtained peak response modes are difficult, we might choose metrics like r.m.s. of displacements or strains, or fatigue damage, in which case we require the capability to obtain the corresponding theoretical estimates. In such scenarios, these quantities may be compared and the error between them minimized.

4. Lift coefficient database extraction formulated as an optimization problem

The systematic modification of C_{lv} and C_m (to allow for warping and second peak) proposed in Section 2.1 can be performed by first parameterizing the relevant features of the databases using a chosen set of parameters $\vec{p}$. Thus, the C_{lv} and C_m databases are now functions of the parameters $\vec{p}$. Allowing these parameters to be modified causes the databases to be flexible and to be a function of the parameters as represented by $C_{lv}(V_r, A^*, \vec{p})$ and $C_m(V_r, A^*, \vec{p})$. This flexible database representation can absorb the information from experiments. More details on parameterizing the databases are given in Section 4.1.

We aim at developing a systematic method for varying this set of parameters $\vec{p}$ such that the prediction using the modified databases (functions of the parameters) matches the experiments. This problem can be viewed as a standard inversion problem of *parameter estimation*, where a *nonlinear forward model* given in Section 4.2 is to be fitted on to *experimental data* of the form $Y_{n-\mathrm{ex}}(z; U(z))$ and $\omega_{n-\mathrm{ex}}(U(z))$. The optimal choice of parameters also requires an appropriate *error metric* $J(\vec{p})$ and an appropriate solution technique which will minimize $J(\vec{p})$ during the solution process. The solution thus obtained is a new optimal set of parameters $\vec{p}_{\mathrm{opt}}$ which minimizes the error metric.

4.1. Parameterization of lift coefficient databases

The parameterization should be such that the features of the databases relevant to the prediction of riser VIV are made flexible using the least number of parameters $\vec{p}$. Numerous parameterizations of the C_{lv} and C_m databases were considered. These included representing the C_{lv} and C_m databases in an analytical form, representing C_{lv} and C_m as Bezier surfaces [refer to Patrikalakis and Maekawa (2002)] with the control points as the parameters, representing C_{lv} and C_m using a set of B-spline basis functions, representing C_{lv} and C_m as meshed surfaces with each data point as a parameter and several combinations of these. All these methods suffer from some or several limitations, the most common being the required number of parameters and the required amount of flexibility. The eventual choice of parameterization is described below.

C_{lv} database parameterization. Based on the observations from a careful study of the SDOF system (flexibly mounted rigid cylinder), the most important feature of the C_{lv} database was found to be the $C_{lv} = 0$ contour (all the free vibration rigid cylinder results align along this curve). Hence, any chosen parameterization of C_{lv} should be such that this contour can be made flexible.

Thus, the C_{lv} database is parameterized using nine parameters which reflect these important features. The definitions of these parameters are produced in Table 1 and are also illustrated in Figs. 4(a) and (b). The first six parameters (p_1 to p_6) allow for describing the warping transformations of the nominal C_{lv} database, to take into account the corrections due to Reynolds number effects. Parameters p_7, p_8 and p_9 allow us to specify the location of a second peak (depicted as a binormal distribution) in the C_{lv} database and to compensate for the motions in the in-line direction. This modification of the nominal C_{lv} database to a new $C_{lv}(V_r, A^*, \vec{p})$ is obtained after making the appropriate transformations in the $V_r - A^*$ domain.

The nominal values of the C_{lv} parameters (represented by $\vec{p}_{\mathrm{nom}}$) are given in Table 1. Thus, using the nominal values of C_{lv} parameters ($\vec{p}_{\mathrm{nom}}$) will result in the nominal lift coefficient database of C_{lv_N}. Thus, corresponding to a modified parameter-set $\vec{p}$, we obtain the modified database of $C_{lv}(V_r, A^*, \vec{p})$. Fig. 5(a) shows an example where the nominal C_{lv_N} database and the modified C_{lv} database (refer to Fig. 5(b)) obtained when only one of the parameters p_3 is modified from its nominal value of $p_{3-\mathrm{nom}} = 5.4$ to a modified value of $p_3 = 7.2$.

Table 1
Definition of the parameters p_1 to p_9 corresponding to the C_{lv} database and their nominal values.

$\vec{p}$	Description of parameter	Nominal value
p_1	Intersection of $C_{lv} = 0$ contour and the V_r-axis corresponding to the lowest V_r	$p_{1-\mathrm{nom}} = 2.94$
p_2	Intersection of $C_{lv} = 0$ contour and the V_r-axis corresponding to the second lowest V_r	$p_{2-\mathrm{nom}} = 4.36$
p_3	Intersection of $C_{lv} = 0$ contour and the V_r-axis corresponding to the third lowest V_r	$p_{3-\mathrm{nom}} = 5.40$
p_4	Intersection of $C_{lv} = 0$ contour and the V_r-axis corresponding to the fourth lowest V_r	$p_{4-\mathrm{nom}} = 8.93$
p_5	Maximum A^* value taken by the $C_{lv} = 0$ contour	$p_{5-\mathrm{nom}} = 0.84$
p_6	Maximum value of the C_{lv} database	$p_{6-\mathrm{nom}} = 0.78$
p_7	V_r location of the second peak added to compensate for in-line motion	$p_{7-\mathrm{nom}} = 0.0$
p_8	A^* location of thesecond peak added to compensate for in-line motion	$p_{8-\mathrm{nom}} = 0.0$
p_9	Maximum value of the second peak added to compensate for in-line motion	$p_{9-\mathrm{nom}} = 0.0$

Refer to Figs. 4(a) and (b) for an illustration of these parameters.

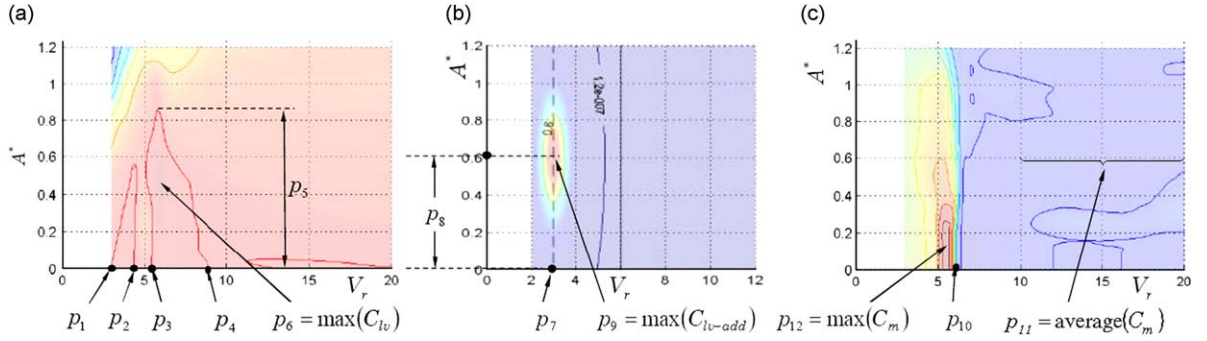

Fig. 4. (a) and (b) depicts parameterization of the C_{lv} database, and (c) depicts parameterization of C_m database. Parameters for correcting in-line motion (b).

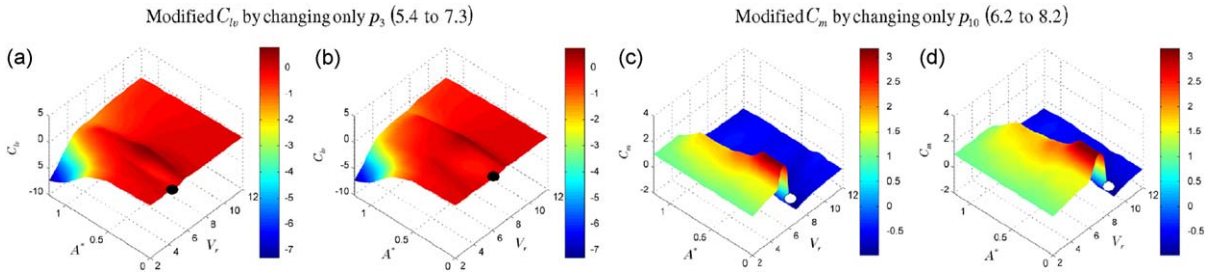

Fig. 5. (a) Nominal C_{lv} database corresponding to the nominal value of parameter p_3 (Nomimal V_r, A^*); (b) example of a modified C_{lv} database obtained by varying the parameter p_3 from its nominal value 5.4–7.3 (Modified V_r, A^*); (c) nominal C_m database corresponding to the nominal value of parameter p_{10} (Nominal V_r, A^*); (d) example of a modified C_{lv} database obtained by varying the parameter p_{10} from its nominal value 6.19–8.2 (Modified V_r, A^*).

C_m database parameterization. The major features important to predicting the VIV response in the C_m database are the sudden transition of C_m corresponding to the Strouhal frequency, the peak C_m value and the asymptotic value attained by the C_m for high flow velocities. Thus the C_m database is parameterized using three parameters (p_{10} to p_{12}) and their definitions can be found in Table 2. The parameters are also illustrated in Fig. 4(c).

The nominal values of the C_m parameters $\vec{p}_{\text{nom}}$ are also given in Table 2. Similar to the C_{lv_N}, using the nominal values of parameters ($\vec{p}_{\text{nom}}$), results in the nominal C_{m_N} database. Again, variations of the parameters from $\vec{p}_{\text{nom}}$ to another arbitrary value $\vec{p}$ will result in a modified database $C_m(V_r, A^*, \vec{p})$. Once again, this modification of the nominal C_{m_N} database to the new $C_m(V_r, A^*, \vec{p})$ database is obtained after making the appropriate transformations in the $V_r - A^*$ domain. Figs. 5(c) and (d) depict an example where the nominal database C_{m_N} and the modified database obtained when only one of the parameters p_{10} is modified from its nominal value of $p_{10-\text{nom}} = 6.19$ to a modified value of $p_{10} = 8.2$.

4.2. Nonlinear forward model

The parametrized $C_{lv}(V_r, A^*, \vec{p})$ and $C_m(V_r, A^*, \vec{p})$ are used to obtain the theoretical estimates of the peak response mode $Y_{n-\text{th}}(z, \vec{p})$ and the peak response frequency $\omega_{n-\text{th}}(\vec{p})$ given the flow profile $U(z)$, boundary conditions, and a set of parameters $\vec{p}$ using the parameterized nonlinear eigenvalue problem (forward model) given by

$$\left\{-\omega^2\left[m + C_m\left(|Y(z)|/D, 2\pi U(z)/(\omega D), \vec{p}\right)\left(\rho_f \frac{\pi D^2}{4}\right)\right] + \mathrm{i}\omega b\right\} Y - \frac{\partial}{\partial z}\left(T\frac{\partial Y}{\partial z}\right) + \frac{\partial^2}{\partial z^2}\left(EI\frac{\partial^2 Y}{\partial z^2}\right) = \mathrm{i}C_{lv}\left(|Y(z)|/D, 2\pi U(z)/(\omega D), \vec{p}\right)\left(\frac{\rho_f U^2}{2} D\right)\frac{Y}{|Y|}. \tag{2}$$

An iterative scheme (VIVA) mentioned previously is employed to obtain these peak response modes $Y_{n-\text{th}}(z, \vec{p})$ and the peak response frequencies $\omega_{n-\text{th}}(\vec{p})$. The above nonlinear eigenvalue problem to predict $\omega_{n-\text{th}}(\vec{p})$ and $Y_{n-\text{th}}(z, \vec{p})$ is called

Table 2
Definition of the parameters p_{10} to p_{12} corresponding to the C_m database and their nominal values.

$\vec{p}$	Description of parameter	Nominal value
p_{10}	The mean value of V_r corresponding to the $C_m = 0$ contour	$p_{10-\mathrm{nom}} = 6.19$
p_{11}	The averaged constant value which C_m takes for large values of V_r	$p_{11-\mathrm{nom}} = -0.54$
p_{12}	The maximum value of the C_m database	$p_{12-\mathrm{nom}} = 3.17$

the *forward model*. The forward model and the parameterization need to be appropriately chosen so that the theoretical model is able to represent the experimental measurements.

4.3. Error metric (optimization index)

We have chosen the peak response mode and peak response frequency as the observable quantities. As a result, we have to take into account the error in both the peak response frequency ω_n and the peak response mode $Y_n(z)$. To reflect the error in frequency and span varying amplitude we choose the following *optimization index* or *error metric* as

$$J(\vec{p}) = \varpi \ \mathrm{rms}\ \{|Y_{n-\mathrm{th}}(z,\vec{p})| - |Y_{n-\mathrm{ex}}(z)|\} + |\omega_{n-\mathrm{th}}(\vec{p}) - \omega_{n-\mathrm{ex}}|, \tag{3}$$

where ϖ is a factor which allows one to weigh the relative importance of reducing the error in peak response frequency or the error in peak response mode. An alternate choice of the error metric was explored and that takes into account the normalized modal magnitudes as

$$J(\vec{p}) = \mathrm{rms}\left\{\frac{|Y_{n-\mathrm{th}}(z,\vec{p})|}{\max_z\{|Y_{n-\mathrm{th}}(z,\vec{p})|\}} - \frac{|Y_{n-\mathrm{ex}}(z)|}{\max_z\{|Y_{n-\mathrm{ex}}(z)|\}}\right\} + \varpi_2|\omega_{n-\mathrm{th}}(\vec{p}) - \omega_{n-\mathrm{ex}}|, \tag{4}$$

where ϖ_2 is a factor which allows one to weigh the relative importance of the peak response frequency and normalized peak response mode.

4.4. Choice of solution technique and computational framework

The choice of the solution technique (optimization method) and the overall computational framework we developed for solving the problem at hand are discussed below.

4.4.1. Choice of solution technique

The solution technique should be chosen, taking into account the conflicting demands of accuracy and speed. Computational resources available to us were two personal computers (PC): PC1 with two processors at 3 GHz each, 1 GB memory, and Windows XP operating system; PC2 with four processors at 2.4 GHz each, 3 GB memory and Windows Vista operating system. A single evaluation of the optimization index $J(\vec{p})$ requires around 30 s of computational time. Thus, in 24 h, approximately 2900 evaluations of the error metric are possible.

The problem at hand consists of an optimization involving 12 parameters (unknowns) which are elements of $\vec{p}$. The large number of parameters in $\vec{p}$ renders *grid search* or *random search* methods computationally impossible. On the other hand, the forward model is nonlinear and it uses parameterized empirically obtained C_{lv} and C_m databases. The forward model (VIVA) is also built using several heuristics like strip theory, power balance, and spatial correlation which often results in sudden changes (discontinuous) in the choice of the peak response frequency and the peak response mode. As a result, our choice of error metric $J(\vec{p})$ is nonlinear (due to the nonlinear forward model) and could be discontinuous. Hence, a *gradient-based* method (*quasi-Newton*) is not expected to work.

For such scenarios, a directed random-search method, like simulated annealing or genetic algorithms, is often recommended and used [refer to Morgan and Rao (2006)]. Such methods allow a compromise of speed and accuracy. For the problem at hand, a variant of the simulated annealing method was chosen due to its simplicity in addition to the performance characteristics. For a detailed discussion on simulated annealing method refer to Morgan and Rao (2006) or Mukundan et al. (2008a). The input to a simulated annealing algorithm is a range for each parameter within which the solution is expected to lie, and the output is the parameter-set $\vec{p}_{\mathrm{opt}}$ which minimizes the error metric over the parameter range.

4.4.2. Computational framework

The Matlab programming environment was employed for the overall scheme mainly due to the ease of programming, built-in libraries, and visualization routines. The first major part of the overall scheme was to develop the simulated annealing code. The simulated annealing code requires several evaluations of the error metric $J(\vec{p})$ corresponding to various parameter-sets $\vec{p}$.

Another set of Matlab code was developed to obtain the modified $C_m(V_r, A^*, \vec{p})$ and $C_{lv}(V_r, A^*, \vec{p})$ databases corresponding to a given parameter-set $\vec{p}$. The sequence of steps involved in evaluating one instance of the optimization index is given as a flowchart depicted in Fig. 6. Each evaluation of the optimization index involves invoking VIVA, for which the modified $C_m(V_r, A^*, \vec{p})$ and $C_{lv}(V_r, A^*, \vec{p})$ databases are first written in a file in the format required by VIVA, which is then called from within the Matlab code. The output from VIVA ($\omega_{n-\mathrm{th}}(\vec{p})$ and $Y_{n-\mathrm{th}}(z, \vec{p})$) is then read by the Matlab code and the corresponding error metric $J(\vec{p})$ is evaluated. VIVA together with the Matlab code provide a framework for systematically varying the modified lift coefficient databases as required by the simulated annealing methodology.

The developed algorithm was thoroughly tested using benchmark datasets to verify its speed and accuracy. The same dataset used for benchmarking the response reconstruction, mentioned in Mukundan et al. (2008a), was used to benchmark the optimal data assimilation algorithm. The benchmark dataset was constructed from one of the VIVA modes. This VIVA mode was generated using a modified lift coefficient database generated by parameter values known *a priori*.

As expected, using the nominal databases for prediction results in significant difference between the experimental and theoretical peak response frequencies and peak response modes as depicted in Figs. 7(a) and (b). This is a condition very similar to the one encountered in real life. The optimal $C_{lv_{\mathrm{opt}}}$ and $C_{m_{\mathrm{opt}}}$ databases are obtained using the simulated annealing methodology and correspond to a parameter-set $\vec{p}_{\mathrm{opt}}$. The results are reproduced in Figs. 7(a) and (b) provides the

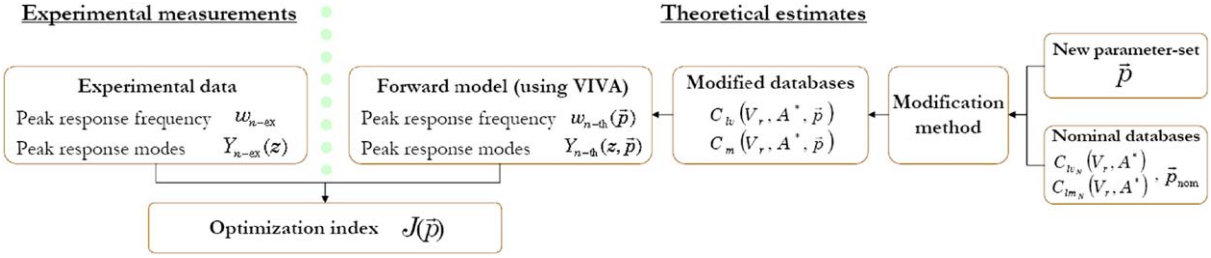

Fig. 6. Flowchart illustrating a single evaluation of the optimization index.

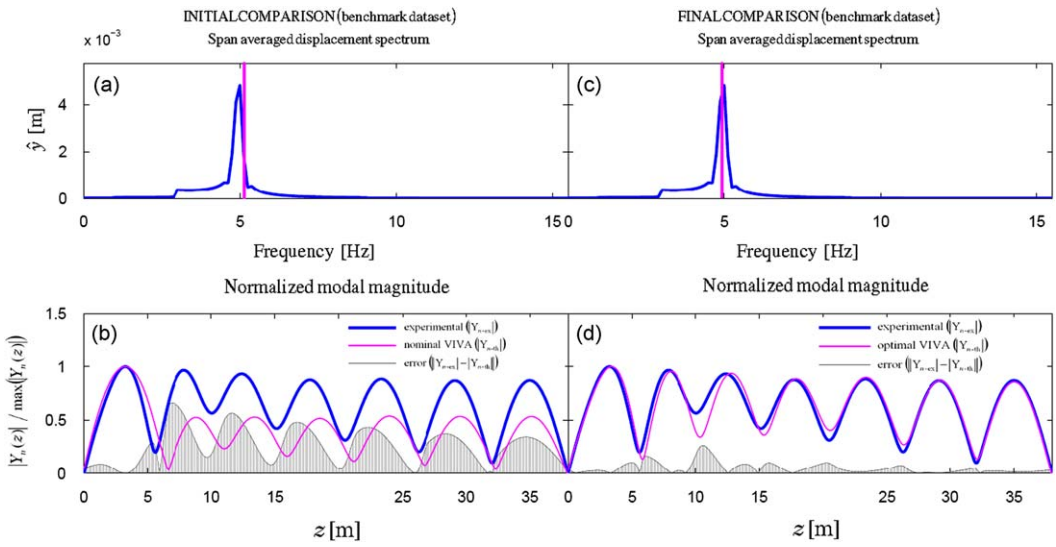

Fig. 7. (a) and (b) depicts a comparison of the experimental and nominal theoretical prediction; (c) and (d) depicts a comparison of the experimental and optimal theoretical prediction.

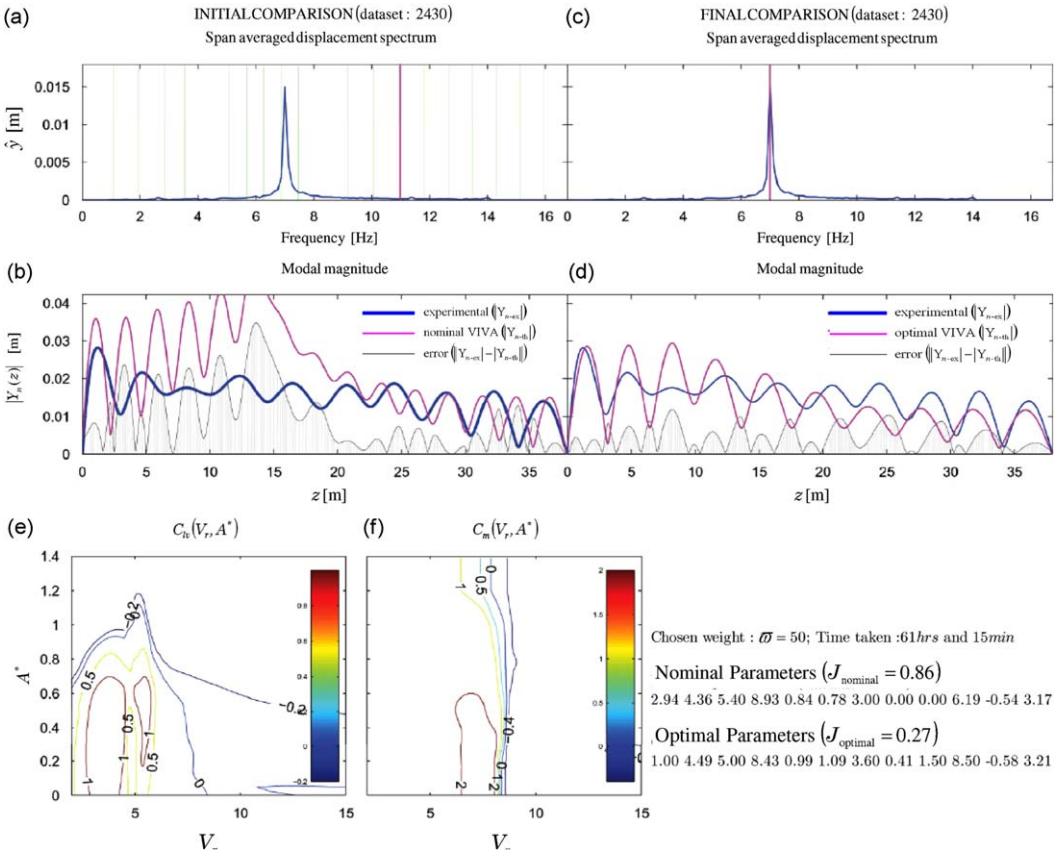

Fig. 8. Application of the optimization method to NDP dataset 2430. (a) and (b) depict a comparison of the experimental and nominal theoretical prediction; (c) and (d) depict a comparison of the experimental and optimal theoretical prediction. Contour plots below (e) and (f) depict the corresponding optimal C_{lv} and C_m databases.

comparison between the experimental data and the prediction using the nominal databases. Figs. 7(c) and (d) provide the comparison between the experimental data and the prediction using the optimal databases. We note that the prediction using the optimal databases (corresponding to $\vec{p}_{\text{opt}}$) closely matches the experimental data, which verifies the applicability of our algorithm. The small differences are attributed to our choice of error metric (and weighing factor ϖ) and the complicated intermediate data processing. The shaded region represents the error in the normalized modal magnitude. The output from such a code is an optimal parameter-set $\vec{p}_{\text{opt}}$ for each of the NDP datasets considered. In addition to the optimal parameter-set, we can also gather parameter-sets for which the error metric is slightly bigger than $J(\vec{p}_{\text{opt}})$.

The method developed is now ready to be applied to the NDP experimental data involving linearly sheared velocity profiles featuring a single peak response frequency. Fig. 8 depicts a typical comparison between the experimental data and the prediction using the nominal databases (a) and (b), and optimal databases (c) and (d) for NDP dataset 2430. We can repeat a similar procedure for all the NDP datasets under consideration and consequently obtain the optimal databases for each such dataset. Contour plots in Figs. 8(e) and (f) depict the corresponding optimal C_{lv} and C_m databases.

5. Universal C_{lv} and C_m databases

As mentioned in the previous section, each NDP dataset yields an optimal parameter-set $\vec{p}_{\text{opt}}$ (or optimal database). Having one different optimal database for each NDP dataset (corresponding to each velocity profile) is inconvenient. In addition, the optimal parameter-set for one NDP dataset may not be the optimal parameter-set for the other NDP datasets. This could be due to the minor (but nonnegligible) data processing errors, due to limitations of empirical models, or due to the internal workings of VIVA. What is required is C_{lv} and C_m databases, which are universal in the sense that they minimize error (in frequency and modal magnitude) for all the NDP datasets under consideration.

We call such databases the *universal databases* and are denoted as $C_{lv_{\text{univ}}}$ and $C_{m_{\text{univ}}}$. The following sections will describe how we obtain the universal databases.

5.1. Obtaining candidate databases (candidate parameter-sets)

First we consider a few selected datasets from the NDP experiments. For each such dataset, we run the simulated annealing (optimization) algorithm several times. Again, for each such run, in addition to the optimal parameter-set, we also collect the parameter-sets where the error metric $J(\vec{p})$ is within a certain percentage of the optimal error metric $J(\vec{p}_{\text{opt}})$, i.e. $J(\vec{p}_{\text{cand}}) \leq [1+\gamma]J(\vec{p}_{\text{opt}})$, where γ (we use $\gamma \approx 8\%$) is a factor which controls the number of candidate parameter-sets isolated from each optimization run. Thus, for each NDP dataset, we have several candidates from various runs of the simulated annealing algorithm. This procedure is repeated now for each of the chosen NDP datasets. The several runs of the simulated annealing algorithm on each NDP dataset increases the probability of finding the best solution. In practice, nearly 8–10 runs are performed on the same dataset. A specific candidate parameter-set is henceforth denoted by $\vec{p}_{\text{cand}_j}$, and around 200 such candidate parameter-sets were isolated.

5.2. Obtaining the best candidate parameter-set

Corresponding to each candidate parameter-set $\vec{p}_{\text{cand}_j}$, we have the associated candidate lift coefficient databases $C_{lv}(V_r, A^*, \vec{p}_{\text{cand}_j})$ and $C_m(V_r, A^*, \vec{p}_{\text{cand}_j})$. Using each of the candidate databases, we evaluate the optimization index for

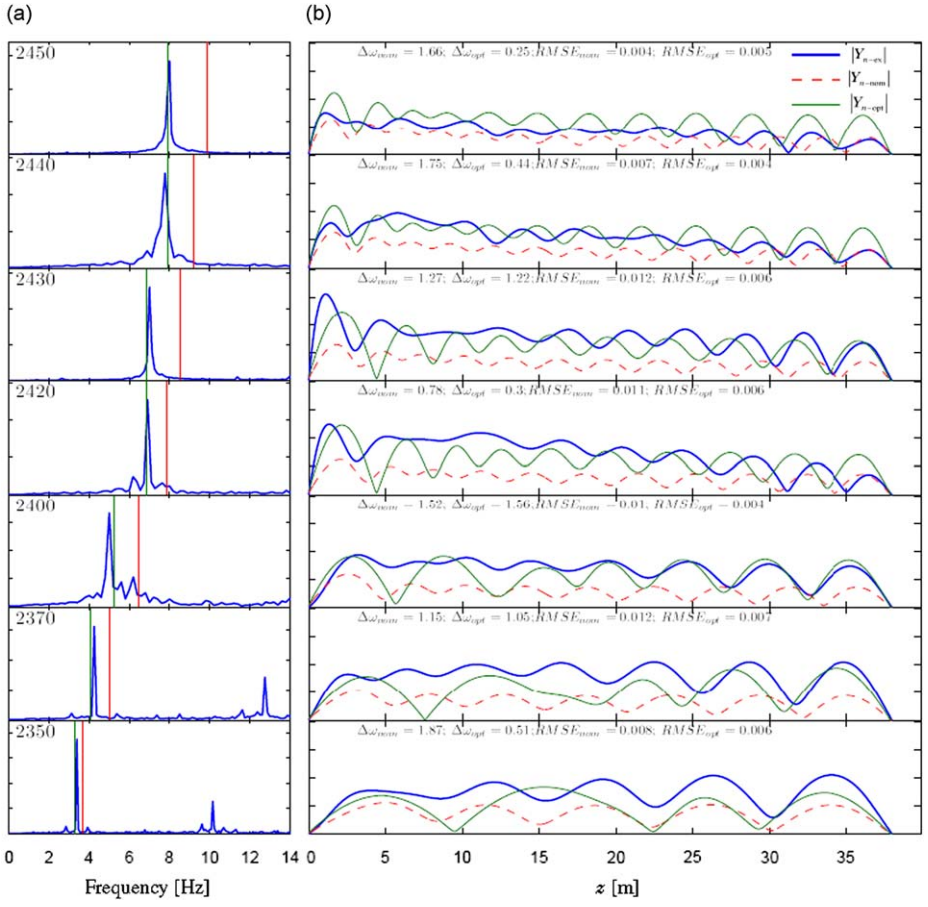

Fig. 9. The predictions of $|Y_n(z)|$ and ω_n using nominal databases (red dashed) and candidate databases $C_{lv}(V_r, A^*, \vec{p}_{\text{cand}_j})$ and $C_m(V_r, A^*, \vec{p}_{\text{cand}_j})$ (green) are compared with the experimentally observed data (blue) for various datasets from the NDP experiments. (a) Span averaged strain spectra and (b) comparison of moda magnitudes of NDP datasets. (For interpretation of the references to color in this figure legend, the reader is referred to the web version of this article.)

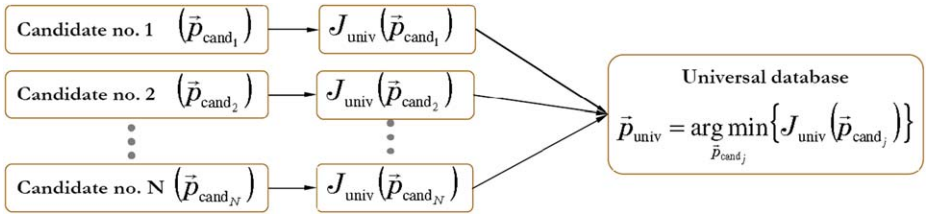

Fig. 10. Flowchart illustrating the process of obtaining the universal parameter-set $\vec{p}_{\text{univ}}$ corresponding to the universal $C_{lv_{\text{univ}}}$ and $C_{m_{\text{univ}}}$ databases.

each NDP dataset (denoted by dataset − i) and we represent it by $J_{\text{dataset-i}}(\vec{p}_{\text{cand}_j})$. Fig. 9 illustrates the results obtained when a typical candidate parameter-set is used to evaluate the error in frequency and the error in modal magnitude for all the considered NDP datasets. Similar figures can be obtained for each candidate parameter-set $\vec{p}_{\text{cand}_j}$. To obtain the candidate which minimizes the overall error for all the datasets we establish the *universal error metric*:

$$J_{\text{univ}}(\vec{p}_{\text{cand}_j}) = J_{\text{dataset-1}}(\vec{p}_{\text{cand}_j}) + J_{\text{dataset-2}}(\vec{p}_{\text{cand}_j}) + \cdots + J_{\text{dataset-i}}(\vec{p}_{\text{cand}_j}) + \cdots. \tag{5}$$

The candidate database which minimizes the universal error metric $J_{\text{univ}}(\vec{p}_{\text{cand}_j})$ is chosen as the universal database (or universal parameter-set $\vec{p}_{\text{univ}}$). That is $\vec{p}_{\text{univ}} = \text{argmin}_{\vec{p}_{\text{cand}_j}}\{J_{\text{univ}}(\vec{p}_{\text{cand}_j})\}$. The procedure followed to obtain the parameter-set $\vec{p}_{\text{univ}}$ corresponding to the universal lift coefficient databases is illustrated in the flowchart given in Fig. 10. The $J_{\text{dataset-i}}(\vec{p}_{\text{cand}_j})$ is evaluated for each NDP dataset corresponding to all the candidate parameter-sets $\vec{p}_{\text{cand}_j}$ that were isolated. Consequently, we obtain the universal error metric $J_{\text{univ}}(\vec{p}_{\text{cand}_j})$ from Eq. (5) for each of the identified candidate parameter-sets. Care should be taken to eliminate certain physically meaningless databases (parameter-sets) from our collection of parameter-sets. Finally, the universal databases $C_{lv_{\text{univ}}}$ and $C_{m_{\text{univ}}}$ which minimize the $J_{\text{univ}}(\vec{p}_{\text{cand}_j})$ are obtained.

5.3. A discussion on the universal C_m database

The *universal added-mass coefficient* database $C_{m_{\text{univ}}}$ is depicted in Fig. 12(a). One important observation is that the characteristic jump in the C_m database has a shift in the reduced frequency $(1/V_r)$. This shift is found to be -0.0295, and remains stable for several runs of the optimization algorithm. As a result, the prediction of the oscillation frequency of the flexible cylinder is expected to be slightly smaller than the predictions using the nominal databases (refer Fig. 14(a)). This observation is in close agreement with the high mode number experiments conducted by Vandiver et al. (2006b) where a reduced frequency in the range of 0.152–0.182 is observed. In addition, as seen from Fig. 11, this apparent reduction in reduced frequency can also be understood from the dependence of Strouhal number on the Reynolds number. The Gopalkrishnan experiments were performed for Reynolds number around 10 000, whereas the present study is based on NDP experiments which were performed at a maximum Reynolds number variation between 16 000 and 46 000. For Reynolds number within the range 16 000–46 000, the corresponding Strouhal frequency is lower than the Strouhal frequency at Reynolds number around 10 000. Thus, the observations from the universal databases are in agreement with the presently available experimental observations. Other modifications include an increase in the maximum value taken by C_m and the width of the peak in the C_m database as shown in Fig. 12(a).

The added mass coefficient C_m is found to produce a significant impact on both the peak response frequency ω_n and also the peak response modal magnitude $|Y_n(z)|$. The importance of C_m on ω_n can easily be deduced from the weak forms of Eq. (1). The impact of C_m on the modal magnitude arises due to the dispersion relation connecting the response frequency ω_n and the wavenumber k_n. The dispersion relation contains the C_m term in addition to linear density m and stiffness terms T and EI.

5.4. A discussion on the universal C_{lv} database

The *universal lift coefficient in phase with velocity* database $C_{lv_{\text{univ}}}$ is depicted in Fig. 12(b). As mentioned earlier, the $C_{lv} = 0$ contour is an important feature of the C_{lv} database. The two resonant lobes (primary and secondary excitation regions) observed in the nominal C_{lv_N} database are seen to merge together to create one large region of $C_{lv} > 0$ in the universal $C_{lv_{\text{univ}}}$ database. In addition, the area of the resonant peaks seems to have spread out over a larger region of

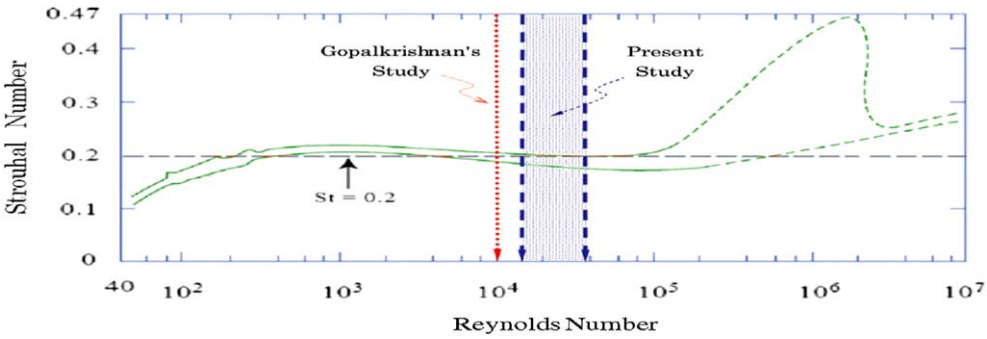

Fig. 11. Strouhal number variation as a function of the Reynolds number, also depicts the Reynolds number corresponding to the Gopalkrishnan database (Reynolds number = 10 000) and the present study (maximum value of Reynolds number in the range 16 000–46 000). For the range of Reynolds number in the present study, the Strouhal number is expected to be lower than that for Reynolds number around 10 000. This figure is adapted from Achenbach and Heinecke (1981), Lienhard (1966), Roshko (1955), Triantafyllou (2006).

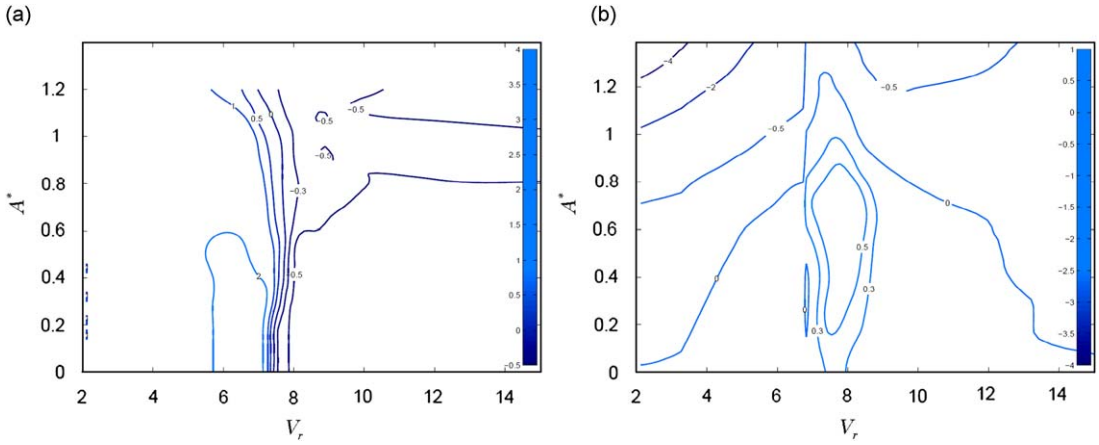

Fig. 12. (a) Depicts the universal $C_{m_{\text{univ}}}$ database ($C_m(V_r, A^*)$) and (b) the universal $C_{lv_{\text{univ}}}$ database ($C_{lv}(V_r, A^*)$) obtained from the optimization code in conjunction with VIVA. A total of nine datasets from NDP experiments (for linearly sheared flow profiles) were used. The maximum value of Reynolds number lies between 16 000 and 46 000.

the V_r axis. This may be explained as follows: VIV of flexible cylinders is fundamentally different from VIV of elastically mounted rigid cylinders, where some parts of the riser may be forced to oscillate due to the excitation produced at another parts. This phenomenon could result in a C_{lv} database which may be much less sensitive to the sharp valley separating the two resonant peaks. Thus, it is not necessary that the span-varying amplitude ratio of riser VIV lie close to the $C_{lv} = 0$ contour line and may result in some averaging resulting from vibrations forced from other locations along the riser.

The maximum A^* value ($A^* \approx 1.24$), taken by the $C_{lv} = 0$ contour, is much higher than the value taken by the nominal C_{lv} database of $A^* \approx 0.8$. Similar observations may be seen from independent experiments performed by Vikestad as mentioned in Larsen et al. (2005) (refer to Fig. 13(b)) using a freely oscillating cylinder which shows a significantly larger response with A^* reaching values as high as 1.15. The results for freely vibrating cylinders by Smogeli et al. (2003) (refer Fig. 13(a)) once again depict a similar trend of high A^* values.

Another important feature of the C_{lv} database is the slope of the $C_{lv}(V_r, A^*)$ surface in the A^* direction corresponding to the resonant frequency. This slope corresponds to the linearized hydrodynamic damping (referred to as b_h) in the empirical model. The universal C_{lv} database has a slope ($b_h \approx 1.32$) which is lower than the slope in the Gopalkrishnan database of ($b_h \approx 1.7$). Thus, the transition from $C_{lv} > 0$ to $C_{lv} < 0$ near the resonant frequency is found to be much less drastic than the observation by Gopalkrishnan.

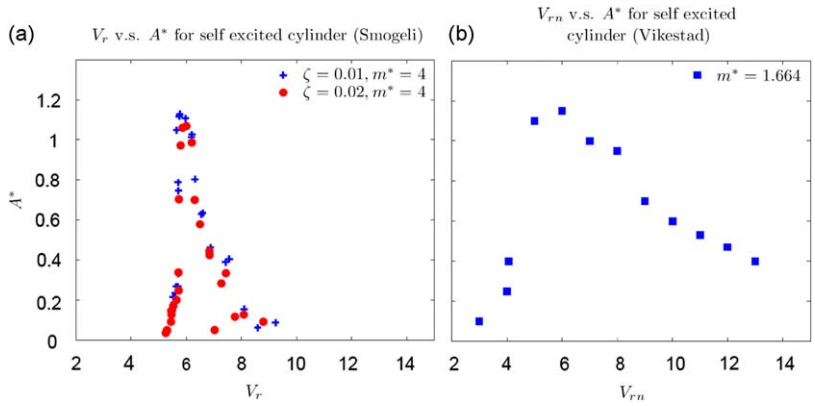

Fig. 13. VIV amplitude of an elastically mounted freely oscillating cylinder in uniform flow. (a) Experiments conducted by Smogeli et al. (2003) for various values of reduced velocity V_r; (b) experiments conducted by Vikestad [refer to Larsen et al. (2005)] for various values of nominal reduced velocity V_{rn}. Note that the amplitude ratio A^* takes values as high as 1.15.

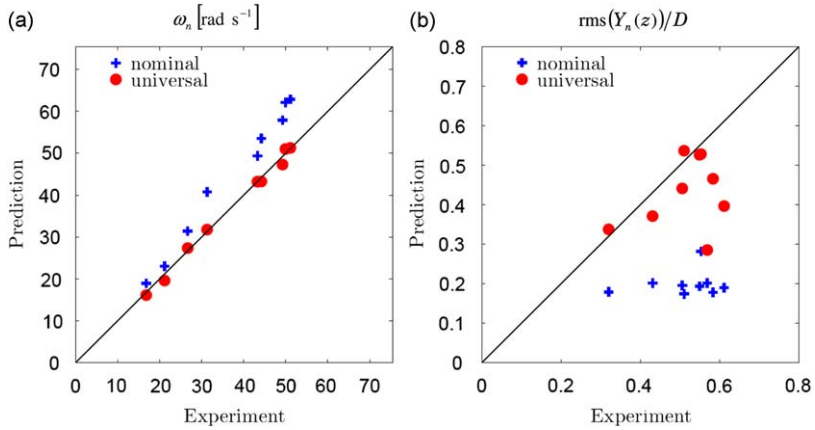

Fig. 14. A snapshot of the results from the use of the universal database with VIVA (for linearly sheared flow profiles). The figure compares experimental and theoretical prediction using nominal (+ symbol) and universal (• symbol) lift coefficient databases for various linearly sheared flow profile datasets from NDP experiments. The use of universal databases improves our estimate of both the peak response frequency (illustrated in (a)) and the peak response modal magnitude (illustrated in (b)). The agreement between the experiments and the predictions using the universal databases result in 44% reduction in error.

5.5. *A discussion on the optimization method and practical issues*

The method presented above addresses several concerns regarding the empirical databases, but these improvements are by no means complete. This section presents some of the valuable insights gained during our attempt to significantly reduce the error in the present prediction methods by improving the empirical lift coefficient databases.

We have assumed that the empirical models for VIV prediction to be accurate, and that the uncertainty in predictions stems from the empirical databases of C_{lv} and C_m alone. However, several researchers, including Jauvtis and Williamson (2004) and Dahl et al. (2006), have observed that allowing IL motions has a significant impact on the CF motions. The ultimate solution seems to be a coupled analysis that takes into account both CF and IL motions. Since such a model has not yet evolved, our method presents the best alternative available to date. As observed from various tests performed (refer to Fig. 14), the universal databases $C_{lv_{\text{univ}}}$ and $C_{m_{\text{univ}}}$ provide significant enhancement in our prediction capability compared to the nominal databases C_{lv_N} and C_{m_N}.

Ideally, we would like to obtain a universal parameter-set by minimizing J_{univ} over the range of parameters. However, in practice, evaluating the J_{univ} is prohibitive. Even if we consider only 10 separate datasets from the NDP experiments, each evaluation of J_{univ} would require 10 runs of VIVA and consequently 10 times the time required to evaluate J.

This would make the present algorithm extremely time consuming and hence impractical. Instead, we perform a two-step strategy of collecting a reduced set of candidate parameters and then choosing the best among them. This two-step strategy is also advantageous in the sense that it allows parallelization by letting us employ several PCs to independently obtain the candidate parameter-sets.

With improving computational abilities, it is expected that our optimization framework can be used in a wide variety of contexts including more complicated parameterizations of the databases, improved empirical models, several datasets from a wide variety of environments, and faster and more accurate optimization algorithms. It is also expected that the framework developed in this paper will also act as a model for testing new VIV modeling techniques.

Another point of interest is our choice of parameters to represent the C_{lv} and C_m databases. In fact, neither this parameterization nor our choice of parameters is unique. Of the various parameterizations considered, the parameterization used was found to best accommodate the conflicting requirements of minimum number of parameters and accurate representation of C_{lv} and C_m. Our choice of parameterization is based on accurately representing the features of C_{lv} and C_m databases which determine the solutions of an elastically mounted rigid cylinder under a constant current. However, the VIV of flexible cylinders (risers) is fundamentally different from the VIV of elastically mounted rigid cylinders. It is not necessary that the span-varying amplitude ratio of vortex-induced vibration of the riser lies close to the $C_{lv} = 0$ contour line. As a result, the parameterization we have chosen may not be adequate in representing all the features of the riser VIV response.

Lastly, all of our analyses are based on linearly sheared cases of NDP data where the harmonic part of vortex-induced response shows only one peak frequency. Introduction of additional frequencies into the riser motions typically results in diffusion of energy between the participating frequencies and may result in cancelations [refer to Sarpkaya (2004)]. In that sense, the use of universal databases may result in more conservative estimates. Evolving a database extraction scheme for multi-frequency response (beating motion) is much more complicated.

6. Concluding remarks

We have developed a systematic and well-posed method to update the lift coefficient databases using experimental data from risers. The lift coefficient databases are represented in a flexible form, with the information from extensive experiments previously conducted as the backbone. The relevant features of the databases are then made flexible using a set of carefully chosen parameters. An optimization scheme was then developed to obtain the best set of parameters such that the theoretical estimates closely follow the experimental observations.

This scheme when applied to a family of datasets from NDP experiments allows obtaining the universal lift coefficient databases which minimize the overall error. The use of the universal lift coefficient databases within VIVA results in significant improvements in predicting the riser VIV cross-flow response in comparison with the use of the nominal lift coefficient databases.

This method will allow us to absorb information from more realistic field experiments, and is expected to bring in the effects of Reynolds number, and the effects of in-line motion in VIV prediction. The method was developed in such a way that no extensive change in the prediction program (e.g., VIVA) user interface is required.

Another application of the method is to produce calibrated *in situ* fatigue monitoring of marine risers. The live VIV data measured by loggers (sensors) placed on a riser is used to build a customized empirical lift coefficient database, which may subsequently be used to produce accurate riser VIV fatigue predictions.

Acknowledgments

The authors gratefully acknowledge the financial support from the MIT-BP Major Projects Program, monitored by Neil Kitney and Pierre Beynet; as well as the generous permission by the Norwegian Deepwater Programme, provided through Dr Kjetil Skaugset, to use the experimental data on a 38 m riser model.

References

Achenbach, E., Heinecke, E., 1981. On vortex shedding from smooth and rough cylinders in the range of Reynolds number 6×10^3 and 5×10^6. Journal of Fluid Mechanics 109, 239–252.

Braaten, H., Lie, H., 2004. NDP riser high mode VIV tests main report. Main Report No. 512394.00.01, Norwegian Marine Technology Research Institute.

Chaplin, J.R., Bearman, P.W., Cheng, Y., Fontaine, E., Graham, J.M.R., Herfjord, K., Huarte, F.J.H., Isherwood, M., Lambrakos, K., Larsen, C.M., Meneghini, J.R., Moe, G., Pattenden, R.J., Triantafyllou, M.S., Willden, R.H.J., 2005. Blind predictions of laboratory measurements of vortex-induced vibrations of a tension riser. Journal of Fluids and Structures 21, 25–40.

Dahl, J.M., Hover, F.S., Triantafyllou, M.S., 2006. Two-degree-of-freedom vortex-induced vibrations using a force assisted apparatus. Journal of Fluids and Structures 22, 807–818.

Gopalkrishnan, R., 1993. Vortex-induced forces on oscillating bluff cylinders. Ph.D. Dissertation. Massachusetts Institute of Technology, Cambridge, MA, USA.

Govardhan, R., Williamson, C.H.K., 2000. Modes of vortex formation and frequency response of a freely vibrating cylinder. Journal of Fluid Mechanics 420, 85–130.

Hover, F.S., Techet, A.H., Triantafyllou, M.S., 1998. Forces on oscillating uniform and tapered cylinders in crossflow. Journal of Fluid Mechanics 363, 97–114.

Jauvtis, N., Williamson, C.H.K., 2004. The effect of two degrees of freedom on vortex-induced vibration at low mass and damping. Journal of Fluid Mechanics 509, 23–62.

Kaiktsis, L., Triantafyllou, G.S., Özbas, M., 2007. Excitation, inertia, and drag forces on a cylinder vibrating transversely to a steady flow. Journal of Fluids and Structures 23, 1–21.

Khalak, A., Williamson, C.H.K., 1996. Dynamics of a hydroelastic cylinder with very low mass and damping. Journal of Fluids and Structures 10, 455–472.

Khalak, A., Williamson, C.H.K., 1999. Motions, forces and mode transitions in vortex-induced vibrations at low mass-damping. Journal of Fluids and Structures 13, 813–851.

Larsen, C.M., Vikestad, K., Yttervik, R., Passano, E., Baarholm, G.S., 2005. VIVANA Theory Manual. MARINTEK, Trondheim, Norway.

Lienhard, J.H., 1966. Synopsis of lift, drag, and vortex frequency data for rigid circular cylinders. Washington State University, College of Engineering Bulletin No. 300.

Marcollo, H., Hinwood, J.B., 2006. On shear flow single mode lock-in with both cross-flow and in-line lock-in mechanisms. Journal of Fluids and Structures 22, 197–211.

Morgan, F.D., Rao, R.V.N., 2006. Course Notes for Data and Models (12.515). Massachusetts Institute of Technology, Cambridge, MA, USA.

Mukundan, H., 2008. Vortex-induced vibration of marine risers: motion and force reconstruction from field and experimental data. Ph.D. Dissertation. Massachusetts Institute of Technology, Cambridge, MA, USA.

Mukundan, H., Hover, F.S., Triantafyllou, M.S., 2008a. A systematic approach to riser VIV response reconstruction. Journal of Fluids and Structures (Under review).

Mukundan, H., Modarres-Sadeghi, Y., Dahl, J.M., Hover, F.S., Triantafyllou, M.S., 2008b. Monitoring VIV fatigue damage on marine risers. Journal of Fluids and Structures 25, 617–628.

Patrikalakis, N.M., Maekawa, T., 2002. Shape Interrogation for Computer-Aided Design and Manufacturing. Springer, Heidelberg.

Roshko, A., 1955. On the wake and drag of bluff bodies. Journal of Aerospace Science 22, 124–132.

Sarpkaya, T., 1979. Vortex-induced oscillations—a selective review. ASME Transactions Series-E—Journal of Applied Mechanics 46, 241–258.

Sarpkaya, T., 2004. A critical review of the intrinsic nature of vortex-induced vibrations. Journal of Fluids and Structures 19, 389–447.

Smogeli, Ø.N., Hover, F.S., Triantafyllou, M.S., 2003. Force-feedback control in VIV experiments. In: Proceedings of the 22nd International Conference on Offshore Mechanics and Arctic Engineering (OMAE), Cancun, Mexico.

Triantafyllou, G.S., 1998. Vortex induced vibrations of long cylindrical structures. In: Proceedings of 1998 ASME Fluids Engineering Division Summer Meeting (FEDSM98), Washington, DC.

Triantafyllou, M.S., 2006. Course Notes for Design Principles for Ocean Vehicles (2.22). Massachusetts Institute of Technology, Cambridge, MA, USA.

Triantafyllou, M.S., Triantafyllou, G.S., Tein, D., Ambrose, B.D., 1999. Pragmatic riser VIV analysis. In: Proceedings of the Offshore Technology Conference (OTC), Houston, TX, USA.

Vandiver, J.K., 1998. Research challenges in the vortex-induced vibration prediction of marine risers. In: Proceedings of the Offshore Technology Conference (OTC), Houston, TX, USA.

Vandiver, J.K., 2003. SHEAR7 User Guide, Department of Ocean Engineering, Massachusetts Institute of Technology, Cambridge, MA, USA.

Vandiver, J.K., Swithenbank, S., Jaiswal, V., Jhingran, V., 2006a. Fatigue damage from high mode number vortex-induced vibration. In: Proceedings of the 25th International Conference on Offshore Mechanics and Arctic Engineering (OMAE), Hamburg, Germany.

Vandiver, J.K., Swithenbank, S., Jaiswal, V., Marcollo, H., 2006b. The effectiveness of helical strakes in the suppression of high-mode-number VIV. In: Proceedings of the Offshore Technology Conference (OTC), Houston, TX, USA.

Venugopal, M., 1996. Damping and response prediction of a flexible cylinder in a current. Ph.D. Dissertation. Massachusetts Institute of Technology, Cambridge, MA, USA.

Williamson, C.H.K., Roshko, A., 1988. Vortex formation in the wake of an oscillating cylinder. Journal of Fluids and Structures 2, 355–381.